Nonlinear Dynamics and Neuroscience

Izvestiya Vysshikh Uchebnykh Zavedeniy. Applied Nonlinear Dynamics. 2023;31(1)

Article DOI: 10.18500/0869-6632-003025

Ring generator of neuron-like activity with tunable frequency

N. M. Egorov[1,2], *M. V. Sysoeva*[1,2]✉, *V. I. Ponomarenko*[1,3], *M. V. Kornilov*[1,3], *I. V. Sysoev*[1,3]

[1]Saratov Brunch of Kotelnikov Institute of Radioengineering and Electronics of the RAS, Russia
[2]Yuri Gagarin State Technical University of Saratov, Russia
[3]Saratov State University, Russia
E-mail: egorov.n.m.omnis@gmail.com, ✉bobrichek@mail.ru, ponomarenkovi@gmail.com, kornilovmv@gmail.com, ivssci@gmail.com

Received 12.10.2022, accepted 10.11.2022, available online 16.12.2022, published 31.01.2023

Abstract. *The aim* of the work is to build a radiophysical generator of neuron-like activity with a frequency tunable in various ways, corresponding to modern ideas about the structure of the hippocampus and the generation of pathological epileptic rhythms in it. *Methods.* The elements of the generator are radio engineering implementations of the complete FitzHugh–Nagumo neuron and the electronic implementation of a chemical synapse in the form of a sigmoid function with a delayed argument. The simulation was carried out in the SPICE simulator. *Results.* Various ways of introducing delay into the coupling are considered: an ideal delay line, a phase filter with a rheostat, one tunable Bessel filter, and a sequence of non-tunable Bessel filters. For circuit implementation, the approach using a Bessel filter with a rheostat is recognized as optimal as a compromise between simplicity and minimization of signal distortion. The dependences of the oscillation frequency on the number of elements in the ring and the delay time are constructed. The bistability of generation regimes is studied for certain values of the parameters. The effect of inclusion of inhibitory elements (interneurons) in the circuit is considered. *Conclusion.* The constructed ring generator models the experimentally observed properties of the dynamics of epileptic discharge fundamental frequency in limbic epilepsy. It is able to reproduce the occurrence of oscillations as a result of external short-term driving, smooth and sharp frequency tuning, the coexistence of different modes with the same parameters.

Keywords: FitzHugh–Nagumo neuron electronic circuit, neural network, time delayed systems, sigmoid coupling.

Acknowledgements. This study was supported by Russian Science Foundation, grant No. 19-72-10030-P, https://rscf.ru/project/19-72-10030/.

For citation: Egorov NM, Sysoeva MV, Ponomarenko VI, Kornilov MV, Sysoev IV. Ring generator of neuron-like activity with tunable frequency. Izvestiya VUZ. Applied Nonlinear Dynamics. 2023;31(1):103–120. DOI: 10.18500/0869-6632-003025

Introduction

The construction of models reflecting the functioning of real neurons and their groups is of scientific and practical technical interest. For example, in robotics, the concept of a central rhythm generator [1, 2] is actively developing, which is necessary for the implementation of simple movements characteristic of living organisms. When modeling pathological modes of brain functioning, in particular, when modeling epilepsy, the question of the formation of the basic rhythm is also of paramount importance. In this paper, we describe the occurrence and evolution of the fundamental frequency of oscillations in the hippocampus in limbic epilepsy using a ring of a small number of radiophysical oscillators constructed for physiological reasons. Compared with purely mathematical modeling, this approach allows us to approach a biological experiment by a number of criteria: from the point of view of the specifics of measurements, from the point of view of the non-stationarity (thermal heating) of the circuit parameters and their non-identity.

When constructing radio-technical models of neurons, the main approach is the schematic reproduction of mathematical models. This was previously noted in [3–5]. From the many variants of mathematical models of biological neurons [6], the FitzHugh-Nagumo neuron model [7, 8] was chosen. It is a dimensionless simplified version of the Hodgkin-Huxley [9], which reproduces the basic properties of excitation waves. The main reason for researchers' interest in this model is the simplicity of implementing nonlinear functions. This makes it possible to assemble an electronic model on the simplest elements of [10] or relatively quickly implement an ensemble of 10 or more elements [14].

In the work [11], a radio engineering scheme of a simplified FitzHugh-Nagumo neuron with one bifurcation parameter a was developed and implemented «in hardware». See the formula (1). In [12], a simulation model was built consisting of 14 simplified FitzHugh-Nagumo neurons connected by a simple linear coupling (1). This is shown in the original work [11]. In [13], it was demonstrated that the proposed simulation model consistently reproduces the necessary modes with variations in the number of network elements (14, 28 and 56 neurons in the network), the coupling architecture (a different number of positive and negative linear couplings) for ensembles of the same number of elements and the initial phase of external influence. As a result, eight radio engineering ensembles were implemented, each with 14 simplified FitzHugh-Nagumo neurons [14]. The radio engineering experiment showed that the implemented circuits are capable of demonstrating the desired behavior — long quasi-regular transients reproducing various characteristics of epileptiform activity, as previously shown in mathematical modeling [15, 16].

$$\begin{aligned} \varepsilon \dot{u}_i(t) &= u_i(t) - c_i u_i^3(t) - v_i(t) + \sum_{j \neq i} k_{ij} u_j, \\ \dot{v}_i(t) &= u_i(t) + a_i, \end{aligned} \tag{1}$$

where u is a dimensionless fast variable corresponding to the transmembrane potential in the Hodgkin-Huxley dimensional model; v is a dimensionless slow variable similar to the recovery current; t is a dimensionless time; ε is the inertia parameter; a is— a dimensionless parameter that controls the intrinsic dynamics of a neuron; c — integration constant (in our works, always $c = 1/3$); k — coupling coefficient.

In the simplified FitzHugh-Nagumo model, inhibitory coupling are impossible: the coupling with any sign will be exciting, just to varying degrees. Therefore, $k < 0$ was called a negative coupling, $k > 0$ — positive. In the work [17], a scheme of a complete FitzHugh-Nagumo neuron (2) was implemented, with two bifurcation parameters a and b and a radio engineering scheme

of a chemical synapse, which mathematically represents a sigmoid function. The combination of these two innovations is minimally necessary to simulate excitatory and inhibitory coupling.

$$\begin{aligned} \varepsilon \dot{u}_i(t) &= u_i(t) - c_i u_i^3(t) - v_i(t) + \sum_{j \neq i} k_{ij} \frac{1 + \tanh\left(u_j(t)\right)}{2}, \\ \dot{v}_i(t) &= u_i(t) + a_i - b_i v_i(t), \end{aligned} \tag{2}$$

where b is another dimensionless parameter that controls the neuron's own dynamics; k is the coupling coefficient, while the coupling is implemented as a displaced hyperbolic tangent $(1 + \tanh(u))/2$, $k < 0$ corresponds to the inhibitory coupling, $k > 0$ — exciting coupling.

In [18] it was shown that in two hardware-implemented complete FitzHugh-Nagumo neurons connected by sigmoid bonds, different scenarios of oscillation occurrence are possible. A saddle-node bifurcation of the cycle is also possible, leading to the appearance of highly nonlinear limit cycles of large amplitude. Long-lived transients have been found near these bifurcations, which are of particular interest for modeling some metastable phenomena in living systems (sleep and epilepsy) [19].

The purpose of this work is to improve the model (2) by adding a delay in the coupling:

$$\begin{aligned} \varepsilon \dot{u}_i(t) &= u_i(t) - c_i u_i^3(t) - v_i(t) + \sum_{j \neq i} k_{ij} \frac{1 + \tanh\left(u_j(t - \tau)\right)}{2}, \\ \dot{v}_i(t) &= u_i(t) + a_i - b_i v_i(t), \end{aligned} \tag{3}$$

where τ is the delay time. The delay naturally occurs in the synapse during signal transmission between the axon and the dendrite as a result of the finiteness of the ion transport speed and can have a significant impact on the dynamics of the network [20].

1. Radio engineering diagram of a neuron with a chemical synapse

In Fig. 1 a schematic diagram of one complete FitzHugh-Nagumo neuron with a synapse is presented. Unlike the mathematical model (3), the parameters of the radio circuit are dimensional. The time parameters can be calculated as $E = R11C1$ and $T = R7C2$.

Let the dimensional values of the mathematical dimensionless variables u and v be denoted as U and V in the scheme. The parameter ε is calculated as $\varepsilon = E/T$. Parameters $c = (R3 + R4)/R3$ and $b = R6/\left(R5 + R_b \cdot \frac{B}{100\%}\right)$ (B — the value expressed as a percentage on the potentiometer R_b) are the scaling factors in U and V. The coupling coefficient k is calculated as $k = R13/R_{IN}$, where R_{IN} is the nominal value on one of the input resistors from $R14$ to $R18$. The parameter a is set by the voltage at the '+"terminal of the U3B amplifier. The total voltage drop on the series-connected resistor $R10 = 5$ kOhm and the potentiometer $R_a = 1$ kOhm is equal to $U_a = 15$ V.

Thus, the entire voltage drop range on the potentiometer is 2.5 V. If the potentiometer is set to $A = 0\%$, the '+"terminal of the U3B amplifier will be exactly 2.5 V. If the potentiometer is set to $A = 100\%$, this voltage is zero. So, the parameter a can be calculated using A, measured in percentages indicated on the potentiometer R_a, as follows: $a = 2.5\left(1 - \frac{A}{100\%}\right)$.

The neuron circuit contains two analog multipliers U1 and U2 and two dual operational amplifiers U3 and U4. Elements U4B and U3A are integrators. They allow you to get U and V. Element U4A — is an inverter that allows you to receive $-U$. The U3B element is a repeater. Multipliers U1 and U2 allow you to build U into a cube according to the formula (3).

The chemical synapse circuit consists of two parts: a circuit that implements a sigmoid function (a radio engineering implementation of a hyperbolic tangent), and a circuit that simulates

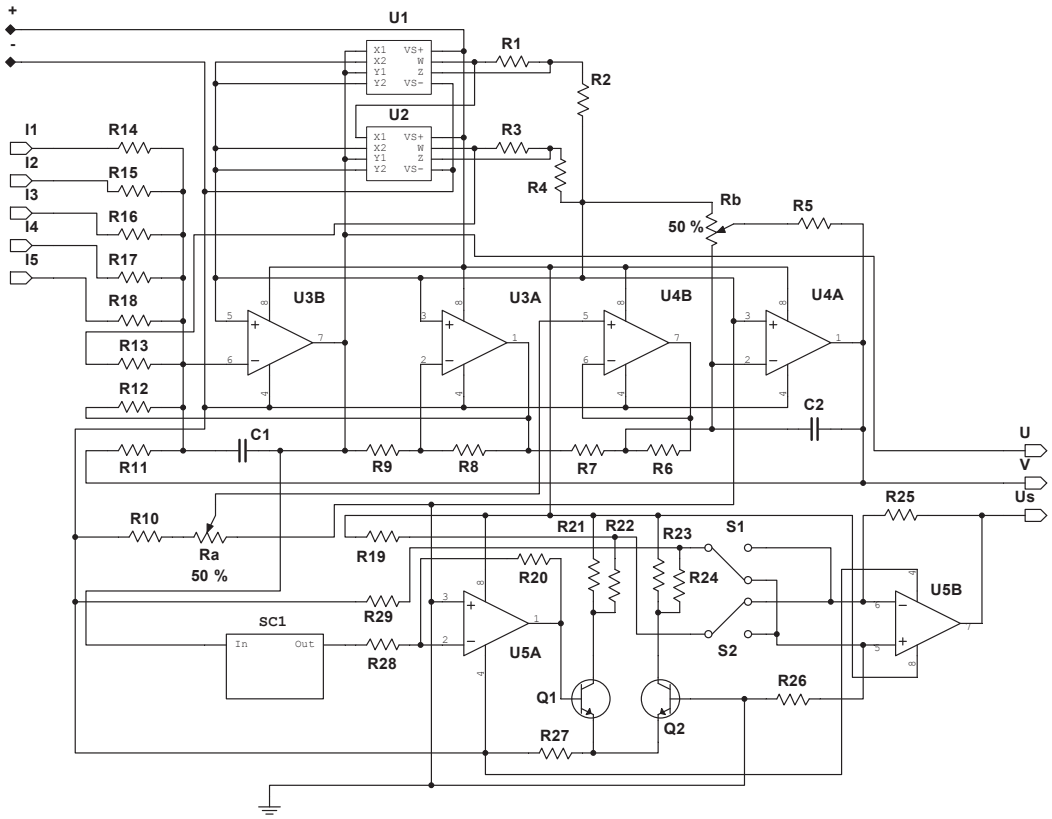

Fig. 1. Circuit diagram of a single complete FitzHugh–Nagumo neuron with synapse. $R1 = R3 = 1$ kΩ, $R2 = 9$ kΩ, $R4 = 2.333$ kΩ, $R5 = 51$ kΩ, potentiometer $R_b = 4.7$ MΩ, $R6 = R7 = R8 = R9 = R11 = R12 = R13 = 100$ kΩ, $R10 = 5$ kΩ, potentiometer $R_a = 1$ kΩ, $R14 - R18$ depends on coupling strength k, $C1 = 1$ nF, $C2 = 0.01$ μF, U1, U2 are multipliers of the type AD633, and U3, U4 are amplifiers of the type AD822. $R19 = R29 = 300$ kΩ, $R20 = 0.51$ kΩ, $R21 = R23 = 1$ kΩ, $R22 = R24 = R28 = 10$ kΩ, $R25 = R26 = 5.1$ kΩ, $R27 = 2$ kΩ, Q1, Q2 are bipolar junction transistors of the type 2N1711, U5 is an amplifier of the type NE5532AI. S1 and S2 are single-pole double-throw switches. They are necessary in order to be able to choose an exciting or inhibitory coupling. SC1 is a subcircuit modeling analog delay

an analog delay. The first circuit contains a dual operational amplifier U5 and two bipolar transistors Q1 and Q2. The inverting amplifier U5A has a gain of 0.05. The differential amplifier U5B has a gain of 0.5. The difference between excitatory and inhibitory coupling is realized by switches S1 and S2. The circuit simulating analog delay will be discussed in detail in the next section.

In Fig. 2 it is shown that there is a time lag between the signal at the input of the neuron and the output of the synapse. This is because the neuron circuit contains inertial elements (capacitors). The time lag caused by the inertia of the circuit depends on the parameters of the model, including the coupling strength. If we measure the time shift that occurs when a signal passes through the neuron circuit, with parameters that will be used in all the experiments described in the article, we get $\Delta t_{\text{neuron}} \approx 60$ microseconds.

According to Fig. 2 it is difficult to determine whether the scheme of the sigmoid function gives some kind of time shift, since the waveform is greatly distorted. In order to understand whether there is inertia in the coupling at the frequencies under consideration, an impact was applied from the harmonic signal generator to the sigmoid function circuit and the response was measured, and then the phase of the initial impact and the phase of the frequency component of the response at the same frequency were compared. The experiment showed that these phases are

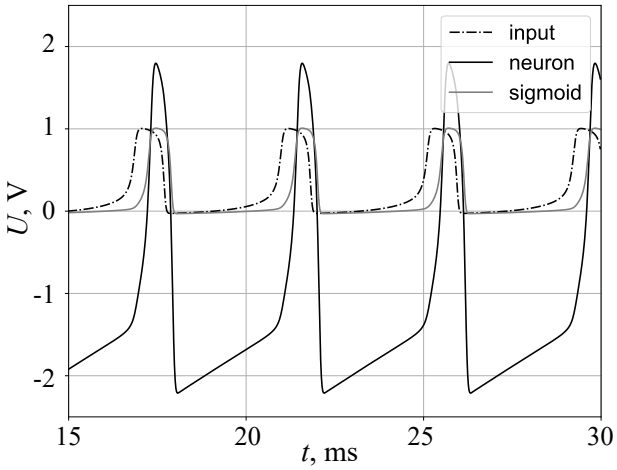

Fig. 2. Time series of a input signal at neuron circuit (dashed dotted line), of an output signal at neuron circuit (solid black line) and of an output signal at sigmoid coupling function circuit (solid gray line)

identical up to the fourth sign. This means that the nonlinear scheme itself, which implements the hyperbolic tangent, does not introduce any inertia.

Further, similar measurements were made already when a signal from a neuron, not a sine wave, was applied to the tangent circuit. As a result, it was shown that the phase at the main frequency of generation varies slightly. This corresponds to a time shift of $\Delta t_{\text{sigmoid}} = 14$ microseconds measured by the maxima in the signal. This shift is due to the non-linearity of the element and the change in the ratio between harmonics (power redistribution), when higher harmonics are amplified at the expense of lower ones (power pumping occurs). At the same time, the phase at high harmonics changes under the influence of the phase of the terms originating from the low-frequency components when they are multiplied. Thus, all the inertia inherent in the contour comes from the circuit of the neuron itself.

2. Implementation of an analog delay line

In this paper, four variants presented in the Fig. 3 were compared to simulate analog delay.

The first variant (Fig. 3, *a*) was used as a reference. This is a standard DELAY component from the National Instruments Multisim radio simulator, which simulates an ideal delay (Fig. 3, *a*). This component stores all input data covering the time period corresponding to the delay time τ. Then it outputs the data according to the FIFO rule: first in — first out. Linear interpolation is used to calculate values that are between time points. The input and output voltage are tied to the ground.

The second option (рис. 3, *b*) is a first-order phase filter. Sometimes it is called an all-pass filter from the English all-pass filter. This filter passes all frequencies of the signal with equal gain, but adds a linear phase shift to each frequency component. By doing this, it contributes to the constant time delay of [21]. Instead of one of the permanent resistors, we put a variable resistor so that we could dynamically change the delay value. This method of implementing a delay line in the system was proposed in [22]. It compares favorably with conventional methods of implementing artificial delay lines consisting of LC links, for example in [23].

The third option (Fig. 3, *c*) is implemented using a Bessel filter. Bessel filters are designed to achieve maximum bandwidth while maintaining a constant group delay. As shown in [24], the Bessel filter is a network with a constant time delay. We chose between Butterworth, Chebyshev

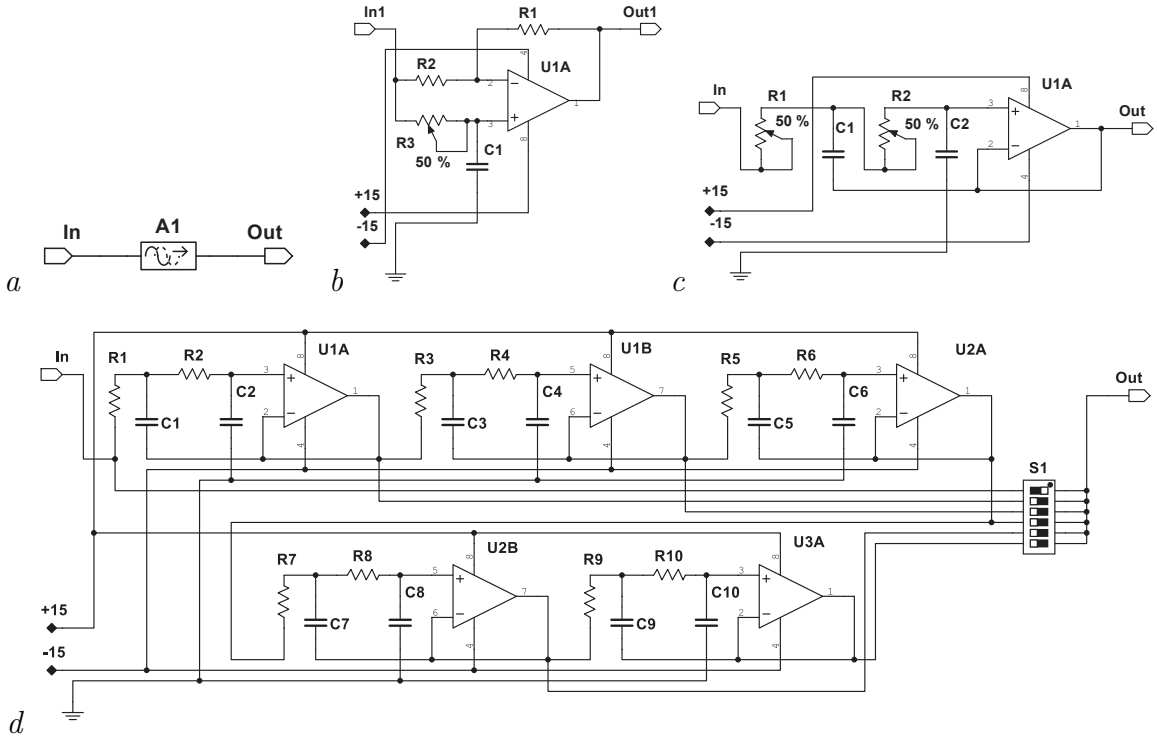

Fig. 3. Implementations of tunable analog delay circuit (subcircuit SC1 content on fig. 1): a — ideal software DELAY; b — all-pass filter with rheostat: $R1 = R2 = 5$ kΩ, $R3 = 50$ kΩ, $C1 = 0.01$ μF, U1A is an amplifier of the type LM358AD; c — Bessel filter with rheostats: $R1 = R2 = 50$ kΩ, $C1 = 5.6$ nF, $C2 = 3.9$ nF, U1A is an amplifier of the type LM358AD; d — sequence of five Bessel filters: $R1 - R10 = 50$ kΩ, $C1 = C3 = C5 = C7 = C9 = 5.6$ nF, $C2 = C4 = C6 = C8 = C10 = 3.9$ nF, $S1$ is a six-position switch; U1, U2, U3 are amplifiers of the type LM358AD

and Bessel filters. We decided to focus on the Bessel filter, since in [25] it was shown that the first two filters have a sudden increase in the time delay near the cutoff frequency.

The fourth option (Fig. 3, d) is a sequence of Bessel filters. Each filter contains constant elements and is set to a delay of $\tau = 0.1$ ms. This variant of the delay line construction is described in [26].

Let's compare the time implementations of signals after passing all four variants of the delay implementation (Fig. 4). We see that when passing the phase filter, the signal is greatly distorted. Five consecutive Bessel filters (0.1 ms delay) distort the signal less than one Bessel filter (0.5 ms delay). In the future, we will face the task of hardware implementation of this scheme. We decided to stop at this option because of the slight difference between the time series at the output of one and five consecutive Bessel filters and because of the significant reduction in the cost of the circuit when using a single Bessel filter with a rheostat. All further calculations were performed for a synapse circuit containing a single tunable Bessel filter.

3. Diagram of a ring generator

Our goal is to obtain a ring generator of neuron-like activity with tunable frequency. To achieve this goal, a block diagram was developed (Fig. 5). One element of this circuit («square») contains a circuit of a neuron with a chemical synapse.

There are two types of neurons in the hippocampus of humans and animals: excitatory

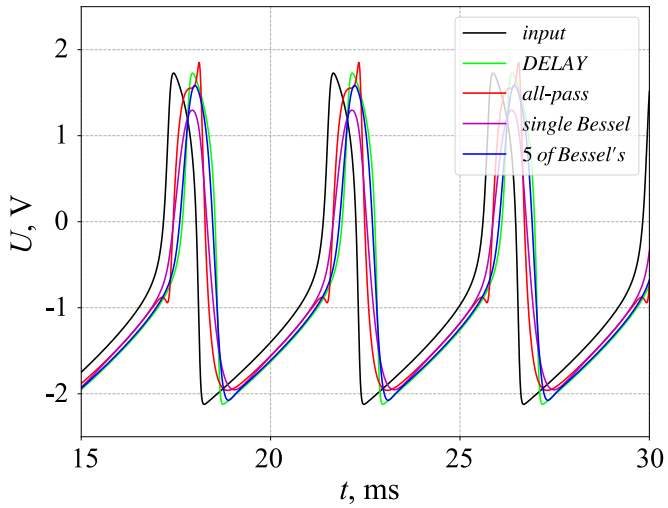

Fig. 4. Comparison of various implementations of the delay $\tau = 0.5$ ms. Black line corresponds to a signal at the input of the loop simulating the delay; green line corresponds to a signal after passing the ideal digital delay; red line corresponds to a signal after passing the phase filter; pink line corresponds to a signal after passing the Bessel filter; blue line corresponds to a signal after passing the sequence of five Bessel filters, with each of which providing a delay of $\tau = 0.1$ ms (color online)

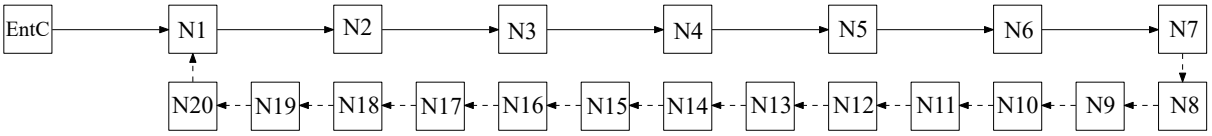

Fig. 5. Block diagram of a ring generator of neuron-like activity with tunable frequency. EntC — external excitatory input (from the pyramidal neuron of the entorhinal cortex $a_{\mathrm{EntC}} = 0.875$, $b_{\mathrm{EntC}} = 0.08$, $k_{\mathrm{EntC}} = 0.6$); N1–N20 — the main neurons of the ring (hypocampal neurons: excitatory pyramidal neurons or inhibitory interneurons ($a_{\mathrm{Hp}} = 1.225$, $b_{\mathrm{Hp}} = 0.08$, $k_{\mathrm{Hp}} = 0.6$ driven by a pyramidal neuron or $k_{\mathrm{Hp}} = -0.6$ when exposed from an interneuron)

pyramidal neurons and inhibitory interneurons. Interneurons are subdivided based on their colocalization with proteins. For example, parvalbumin or cholecystokinin interneurons. They innervate different parts of pyramidal neurons [27]. The hippocampus receives information from the entorhinal cortex. The main information goes through the perforating tract from the second layer of the entorhinal cortex to the granular cells of the dentate fascia (small excitatory neurons). Then, through mossy fibers, information is transmitted to the pyramids and interneurons of the CA3 field of the hippocampus. Then from the pyramids of the CA3 field goes to the pyramids and interneurons of the CA2 and CA1 fields (for more information in [28]).

There is a direct excitatory pathway from the II layer of the entorhinal cortex to the pyramids and interneurons of the CA3 and CA2 regions of the hippocampus and from the III layer of the entorhinal cortex to the pyramids and interneurons of CA1. But less information is transmitted through these tracts than through the dentate fascia. The coupling between the pyramids of the CA1 field are much weaker than between the pyramids of the CA2 and CA3 layers. Interneurons in the hippocampus are only 10%. However, taking into account braking interneurons in both mathematical and radio engineering models is very important. In diseases such as schizophrenia, Alzheimer's disease, temporal lobe epilepsy, the total volume of the hippocampus decreases precisely due to a decrease in interneurons, not pyramidal cells.

In this paper, the functioning of the hippocampal CA1 field is reproduced in a very simplified form after receiving an exciting signal from the third layer of the entorhinal cortex

and with an increase in the number of couplings within the hippocampus. The external input (the pyramidal neuron of the entorhinal cortex) is in oscillatory mode with the parameters $a_{\mathrm{EntC}} = 0.875$ and $b_{\mathrm{EntC}} = 0.08$. Hippocampal neurons are in subthreshold mode with parameters $a_{\mathrm{Hp}} = 1.225$ and $b_{\mathrm{Hp}} = 0.08$. The force of interaction inside the hippocampus and the force of external influence were taken the same $k_{\mathrm{Hp}} = k_{\mathrm{EntC}} = 0.6$.

Two scenarios were considered: 1) the generating ring is composed only of excitatory neurons - pyramids; 2) there may be two interneurons inside the ring in different places, including two in a row. Preliminary experiments have shown that if all neurons are excitatory, then at a maximum delay of 0.5 ms, at least seven neurons are needed for vibrations to begin in the ring. This is the minimum number of neurons that we considered. In Fig. 5 coupling between neurons N1–N7 are represented by solid lines, since these are the main neurons that have always been present in the network, and the rest of the lines are dashed — these neurons are additional and were not present in all experiments.

4. Dependence of the oscillation frequency of the network on the internal parameters of the network

The parameters of the ring neurons used in this work correspond to the subthreshold non-oscillatory mode for each individual neuron. When neurons close in a ring, a time-delayed coupling occurs between them. This delay corresponds in a real biological neuron to a delay in a chemical synapse, which is conditioned by the finite times required for ion transport through the synapse. Then a short-term effect is applied to one of the neurons of the ring with a characteristic oscillation period $T_{\mathrm{EntC}} = 4.129$ ms or an oscillation frequency of approximately $f_{\mathrm{EntC}} = 242$ Hz, the time of external exposure $w = 5\,T_{\mathrm{EntC}}$. This frequency of external influence corresponds to the lowest possible frequency of neuron self-oscillations. The next section will also cover the frequencies above. After the external influence is applied, each individual node of the network begins to generate periodic nonlinear oscillations. These fluctuations are the result of network organization. Their appearance and frequency are determined by the number of nodes in the ring, the delay time in communication and the intrinsic inertial properties of individual neurons, as shown in the mathematical model [29].

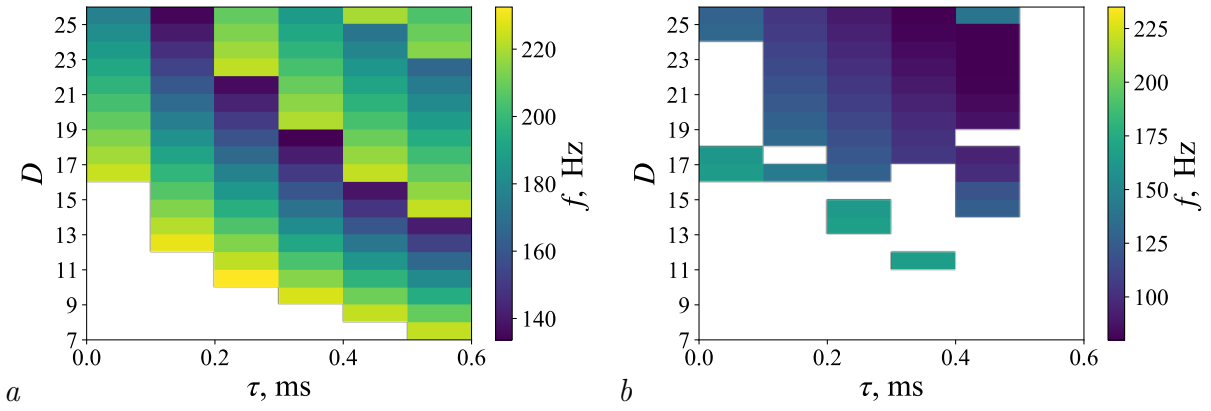

Fig. 6. Dependencies of the main oscillation frequency f in the circuit on the number of elements in the ring D and on the delay time τ. Frequency of external driving is $f_{\mathrm{EntC}} = 242$ Hz. The color indicates the oscillation frequency occurring in the ring. The white color corresponds to the absence of oscillations in the ring. Subplot a corresponds to all excitatory neurons in the circuit, subplot b corresponds a case when two inhibitory neurons (N6 and N16) are included to the circuit (color online)

In Fig. 6 shows the dependence of the fundamental frequency of f oscillations of neurons in the circuit on the number of elements in the ring D and on the delay time τ. If the vibrations in the ring are not triggered, then this option is shown in white. The colored rectangles correspond to different values of the fundamental frequency of oscillations in the ring in case of oscillation triggering. To calculate the fundamental frequency, the period of T_1 oscillations of the neuron N1 was estimated from time series and the frequency was obtained as $1/T_1$. The remaining neurons of the ring generate similar activity, which is uniformly shifted in phase so that the total shift on the entire ring is 2π. The delay τ is postponed along the abscissa axis, which occurs in a separate circuit that simulates an analog delay line. The delay that occurs in the neuron circuit due to the inertia of the circuit was not taken into account when plotting the graph. In Fig. 6 it is shown that even with zero delay τ (if the number of nodes in the ring is large enough) oscillations occur. The reason for this lies in the inertial properties of a single neuron — the presence of a time shift for the signal that passed through the neuron circuit.

Fig. 6, *a* is given for the case when all the neurons in the ring are excitatory. We see that the greater the delay in communication, the fewer neurons are needed in order for vibrations to begin in the entire ring. With the maximum delay we studied $\tau = 0.5$ ms, 7 pyramid neurons are enough for the network to begin to oscillate. If you fix the delay time τ and gradually increase the number of neurons in the network D or fix the number of neurons in the network D and gradually increase the delay time τ (less physiologically), you can see that at first there are fluctuations at a frequency of about 230 Hz, and then, according to As the number of neurons increases, the frequency drops to about 140 Hz. Then, when another neuron is added, a sharp jump occurs and the main oscillation frequency again becomes about 225 Hz, which corresponds to twice the frequency for a given number of elements: two pulses moving simultaneously in the opposite phase, at a distance of half the elements from each other, move through the network. Such a regime turns out to be possible and stable, since the time of refractoriness becomes less than half of the period and the neurons have time to «recover» not for the whole period, but for half. An indirect confirmation of this explanation is that with a delay of $\tau = 0.5$ ms, oscillations at the fundamental frequency begin at the number of neurons $D = 7$, and oscillations with a doubled frequency — at $D = 14$. Further, as the D increases, the frequency begins to fall again. And for $\tau = 0.5$ ms at $D = 21$, the frequency reaches a minimum of $f = 174$ Hz. Then, at $D = 22$, the frequency increases sharply to $f = 219$ Hz — the generator switches to triple frequency mode. Thus, the mode with the maximum possible number of simultaneously running pulses is always preferred, and the «fork» between the minimum and maximum frequencies decreases with an increase in the number of simultaneously coexisting pulses.

Fig. 6, *b* is given for the case when two interneurons (N6 and N 16) are added to the ring. There are no smooth dependencies of f on τ and D. Firstly, not with every combination (τ, D), the network began to fluctuate after the end of the exposure. Secondly, the maximum oscillation frequency of 165 Hz was obtained at all with zero delay. Thirdly, at the maximum studied delay time $\tau = 0.5$ms, the oscillations did not start at any D. Nevertheless, the very possibility of generation even in the presence of two interneurons in the ring (their number in the hippocampus is about 10 times less than the pyramids) shows the fundamental structural stability of the proposed scheme.

5. Dependence of the oscillation frequency of the network on the parameters of external influence

We examined the behavior of the ring generator when changing the parameters of external influence: the frequency f_{Etc}, the duration w and the initial phase φ. As experiments have shown, diagrams (similar to Fig. 6), constructed with different duration and initial phase of exposure, do not differ from each other. But the frequency of external influence significantly changes the situation. The higher the frequency of external influence, the more difficult it is to start vibrations in the ring (we need more τ and D). This is due to the fact that the frequency of exposure is becoming higher and higher than the natural oscillation frequency of the ring neurons, and it is increasingly difficult for them to synchronize: the neurons «get tired» and do not respond due to refractoriness. The same principle underlies the methods of combating epileptic seizures using high-frequency stimulation [30, 31].

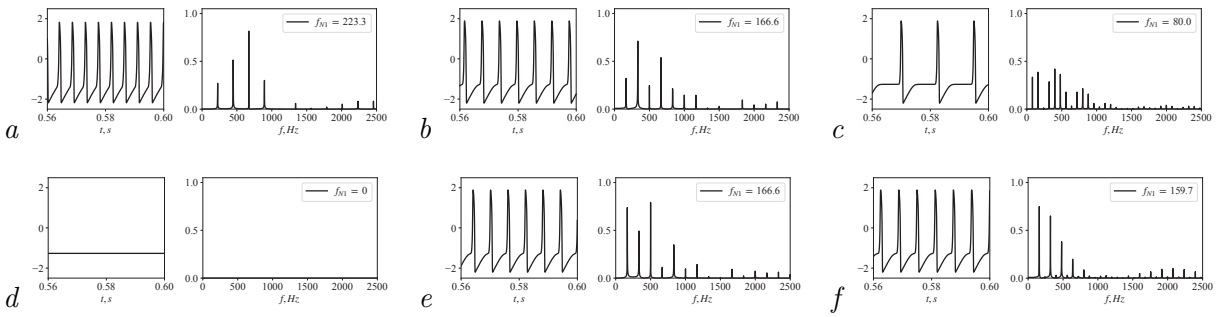

Fig. 7. Time series and amplitude spectra of the N1 neuron for two sets of parameters: $f_{\text{EntC}} = 250.7$ Hz (upper subplots) and $f_{\text{EntC}} = 344.1$ Hz (lower subplots). The number of neurons in the ring is different for different subplots: $D = 7$ (for a and d), $D = 11$ (for b and e), $D = 23$ (for c and f)

The most important thing for us is that by slightly changing the frequency of exposure, but without changing the internal parameters of the ring, it is possible to output the generator to various oscillatory modes. In Fig. 7 shows time series and amplitude spectra taken from neuron N1 at different frequencies of external influence. It can be seen that a ring of 7 neurons at the frequency of external action $f_{\text{EntC}} = 250.7$ Hz is triggered at a frequency of $f_{\text{N1}} = 223.3$ Hz, and at $f_{\text{EntC}} = 344.1$ Hz — does not start at all (fig. 7, a, d). A ring of 11 neurons behaves the same at both considered exposure frequencies (Fig. 7, b, e). But in a ring of 23 neurons at $f_{\text{EntC}} = 250.7$ Hz, oscillations are realized at a frequency of 80.0 Hz (Fig. 7, c). At the same time, at the highest frequency of exposure, vibrations in the ring occur at twice the frequency of 159.7 Hz.

Conclusion

The question of how the main oscillatory rhythms responsible for normal and pathological activity are formed in the brain has been raised and discussed many times [32–34]. The existing attempts to create a general theory are still descriptive in nature [35]. Much attention is drawn to the issues of synchronization of various brain structures [36], including in the application to epilepsy and other pathological conditions [37]. At the same time, the issue of generating the fundamental frequency for most processes has not been solved in principle. For focal epilepsies, it is assumed that the pacemaker is a very small neural ensemble [38] — micro-circuit. At the same time, we know that the generation frequency can be adjusted within wide limits, both smoothly

and in leaps, very individually for each patient or animal [39].

In this work, we managed to create a circuit of a radio-technical ring generator built according to the principles of the organization of the limbic system of mammals. It consists of several model radio-technical neurons and radio-technical synapses in the form of filters that implement lag. The key feature of the generator is that its frequency can be rebuilt in three ways: by changing the delay time (smooth tuning is available in a wide range), by changing the number of elements in the network (the restructuring will be carried out in a leap), due to different frequencies of external influence (in conditions of multistability, coexisting modes with multiple frequencies can be realized). The resulting generator simulates possible mechanisms for the formation of the main frequency of pathological activity in the hippocampus in focal limbic epilepsy. It is important that from a biological point of view, the scheme turned out to be structurally stable: the inclusion in the ring of one or even two interneurons suppressing the activity of the next neuron, instead of exciting pyramids, reduces the generation area in the parameter space (D, τ) — the number of neurons, the delay time — but does not completely eliminate it. This significantly increases the biological relevance of the model, as it significantly increases the probability of the formation of such a ring structure in practice. At the same time, lower-frequency modes are implemented. This further increases the variety of types of oscillatory activity inherent in the generator.

The main purpose of the work was to model a biological object — a pacemaker of limbic epilepsy. However, the constructed generator can probably be used independently as a source of multi-frequency periodic pulse signals.

References

1. Lodi M, Shilnikov AL, Storace M. Design principles for central pattern generators with preset rhythms. IEEE Transactions on Neural Networks and Learning Systems. 2020;31(9):3658–3669. DOI: 10.1109/TNNLS.2019.2945637.
2. Kurkin SA, Kulminskiy DD, Ponomarenko VI, Prokhorov MD, Astakhov SV, Hramov AE. Central pattern generator based on self-sustained oscillator coupled to a chain of oscillatory circuits. Chaos. 2022;32(3):033117. DOI: 10.1063/5.0077789.
3. Mahowald M, Douglas R. A silicon neuron. Nature. 1991;354(6354):515–518. DOI: 10.1038/354515a0.
4. Rasche C, Douglas R. An improved silicon neuron. Analog Integrated Circuits and Signal Processing. 2000;23(3):227–236. DOI: 10.1023/A:1008357931826.
5. van Schaik A. Building blocks for electronic spiking neural networks. Neural Networks. 2001;14(6–7):617–628. DOI: 10.1016/S0893-6080(01)00067-3.
6. Dmitrichev AS, Kasatkin DV, Klinshov VV, Kirillov SY, Maslennikov OV, Shchapin DS, Nekorkin VI. Nonlinear dynamical models of neurons: Review. Izvestiya VUZ. Applied Nonlinear Dynamics. 2018;26(4):5–58. DOI: 10.18500/0869-6632-2018-26-4-5-58.
7. FitzHugh R. Impulses and physiological states in theoretical models of nerve membrane. Biophysical Journal. 1961;1(6):445–466. DOI: 10.1016/S0006-3495(61)86902-6.
8. Nagumo J, Arimoto S, Yoshizawa S. An active pulse transmission line simulating nerve axon. Proceedings of the IRE. 1962;50(10):2061–2070. DOI: 10.1109/JRPROC.1962.288235.
9. Hodgkin AL, Huxley AF. A quantitative description of membrane current and its application to conduction and excitation in nerve. The Journal of Physiology. 1952;117(4):500–544. DOI: 10.1113/jphysiol.1952.sp004764.
10. Binczak S, Jacquir S, Bilbault JM, Kazantsev VB, Nekorkin VI. Experimental study of electrical FitzHugh–Nagumo neurons with modified excitability. Neural Networks.

2006;19(5):684–693. DOI: 10.1016/j.neunet.2005.07.011.
11. Kulminskiy DD, Ponomarenko VI, Prokhorov MD, Hramov AE. Synchronization in ensembles of delay-coupled nonidentical neuronlike oscillators. Nonlinear Dynamics. 2019;98(1):735–748. DOI: 10.1007/s11071-019-05224-x.
12. Egorov NM, Ponomarenko VI, Sysoev IV, Sysoeva MV. Simulation of epileptiform activity using network of neuron-like radio technical oscillators. Technical Physics. 2021;66(3):505–514. DOI: 10.1134/S1063784221030063.
13. Egorov NM, Ponomarenko VI, Melnikova SN, Sysoev IV, Sysoeva MV. Common mechanisms of attractorless oscillatory regimes in radioengineering models of brain thalamocortical network. Izvestiya VUZ. Applied Nonlinear Dynamics. 2021;29(6):927–942 (in Russian). DOI: 10.18500/0869-6632-2021-29-6-927-942.
14. Egorov NM, Kulminskiy DD, Sysoev IV, Ponomarenko VI, Sysoeva MV. Transient dynamics in electronic neuron-like circuits in application to modeling epileptic seizures. Nonlinear Dynamics. 2022;108(4):4231–4242. DOI: 10.1007/s11071-022-07379-6.
15. Kapustnikov AA, Sysoeva MV, Sysoev IV. The modeling of spike-wave discharges in brain with small oscillatory neural networks. Mathematical Biology and Bioinformatics. 2020;15(2):138–147 (in Russian). DOI: 10.17537/2020.15.138.
16. Kapustnikov AA, Sysoeva MV, Sysoev IV. Transient dynamics in a class of mathematical models of epileptic seizures. Communications in Nonlinear Science and Numerical Simulation. 2022;109:106284. DOI: 10.1016/j.cnsns.2022.106284.
17. Egorov NM, Sysoev IV, Ponomarenko VI, Sysoeva MV. Epileptiform activity generation by an ensemble of complete electronic FitzHugh-Nagumo oscillators connected by a sigmoid couplings. In: Proceedings of SPIE. Vol. 12194. Computational Biophysics and Nanobiophotonics. Bellingham: SPIE; 2022. P. 1219403. DOI: 10.1117/12.2623993.
18. Egorov NM, Sysoev IV, Ponomarenko VI, Sysoeva MV. Complex regimes in electronic neuron-like oscillators with sigmoid coupling. Chaos, Solitons & Fractals. 2022;160:112171. DOI: 10.1016/j.chaos.2022.112171.
19. Rabinovich MI, Zaks MA, Varona P. Sequential dynamics of complex networks in mind: Consciousness and creativity. Physics Reports. 2020;883:1–32. DOI: 10.1016/j.physrep.2020.08.003.
20. Wang Q, Perc M, Duan Z, Chen G. Impact of delays and rewiring on the dynamics of small-world neuronal networks with two types of coupling. Physica A: Statistical Mechanics and its Applications. 2010;389(16):3299–3306. DOI: 10.1016/j.physa.2010.03.031.
21. Winder S. Analog and Digital Filter Design. 2nd edition. USA: Elsevier; 2002. 458 p. DOI: 10.1016/B978-0-7506-7547-5.X5000-3.
22. Banerjee T, Biswas D, Sarkar BC. Anticipatory, complete and lag synchronization of chaos and hyperchaos in a nonlinear delay-coupled time-delayed system. Nonlinear Dynamics. 2013;72(1–2):321–332. DOI: 10.1007/s11071-012-0716-4.
23. Srinivasan K, Raja Mohamed I, Murali K, Lakshmanan M, Sinha S. Design of time delayed chaotic circuit with threshold controller. International Journal of Bifurcation and Chaos. 2011;21(3):725–735. DOI: 10.1142/S0218127411028751.
24. Karki J. Active Low-Pass Filter Design. Texas: Texas Instruments; 2000. 24 p.
25. Cao P, Fan H, Wang D, Shu H, Yang B, Han Y, Dong J. Compensation circuit design for tuned half-wavelength transmission lines based on Bessel filter. International Journal of Electrical Power & Energy Systems. 2022;134:107335. DOI: 10.1016/j.ijepes.2021.107335.
26. Buscarino A, Fortuna L, Frasca M, Sciuto G. Design of time-delay chaotic electronic circuits. IEEE Transactions on Circuits and Systems I: Regular Papers. 2011;58(8):1888–1896. DOI: 10.1109/TCSI.2011.2107190.

27. Rudy B, Fishell G, Lee S, Hjerling-Leffler J. Three groups of interneurons account for nearly 100% of neocortical GABAergic neurons. Developmental Neurobiology. 2011;71(1):45–61. DOI: 10.1002/dneu.20853.
28. Vinogradova OS. Hippocampus as comparator: Role of the two input and two output systems of the hippocampus in selection and registration of information. Hippocampus. 2001;11(5):578–598. DOI: 10.1002/hipo.1073.
29. Sysoev IV, Kornilov MV, Makarova NA, Sysoeva MV, Vinogradova LV. Modeling limbic seizure initiation with an ensemble of delay coupled neuroscillator. In: Lacarbonara W, Balachandran B, Leamy MJ, Ma J, Tenreiro Machado JA, Stepan G, editors. Advances in Nonlinear Dynamics. NODYCON Conference Proceedings Series. Cham: Springer; 2022. P. 73–81. DOI: 10.1007/978-3-030-81170-9_7.
30. Nelson TS, Suhr CL, Freestone DR, Lai A, Halliday AJ, McLean KJ, Burkitt AN, Cook MJ. Closed-loop seizure control with very high frequency electrical stimulation at seizure onset in the GAERS model of absence epilepsy. International Journal of Neural Systems. 2011;21(2):163–173. DOI: 10.1142/S0129065711002717.
31. van Heukelum S, Kelderhuis J, Janssen P, van Luijtelaar G, Lüttjohann A. Timing of high-frequency cortical stimulation in a genetic absence model. Neuroscience. 2016;324:191–201. DOI: 10.1016/j.neuroscience.2016.02.070.
32. Lopes da Silva F. Neural mechanisms underlying brain waves: from neural membranes to networks. Electroencephalography and Clinical Neurophysiology. 1991;79(2):81–93. DOI: 10.1016/0013-4694(91)90044-5.
33. Schnitzler A, Gross J. Normal and pathological oscillatory communication in the brain. Nature Reviews Neuroscience. 2005;6(4):285–296. DOI: 10.1038/nrn1650.
34. Benca R, Duncan MJ, Frank E, McClung C, Nelson RJ, Vicentic A. Biological rhythms, higher brain function, and behavior: Gaps, opportunities, and challenges. Brain Research Reviews. 2009;62(1):57–70. DOI: 10.1016/j.brainresrev.2009.09.005.
35. Buzsáki G. Rhythms of the Brain. Oxford: Oxford University Press; 2006. 448 p. DOI: 10.1093/acprof:oso/9780195301069.001.0001.
36. Rudrauf D, Douiri A, Kovach C, Lachaux JP, Cosmelli D, Chavez M, Adam C, Renault B, Martinerie J, Le Van Quyen M. Frequency flows and the time-frequency dynamics of multivariate phase synchronization in brain signals. NeuroImage. 2006;31(1):209–227. DOI: 10.1016/j.neuroimage.2005.11.021.
37. Good LB, Sabesan S, Marsh ST, Tsakalis K, Treiman D, Iasemidis L. Control of synchronization of brain dynamics leads to control of epileptic seizures in rodents. International Journal of Neural Systems. 2009;19(3):173–196. DOI: 10.1142/S0129065709001951.
38. Paz JT, Huguenard JR. Microcircuits and their interactions in epilepsy: is the focus out of focus? Nature Neuroscience. 2015;18(3):351–359. DOI: 10.1038/nn.3950.
39. Sysoeva MV, Vinogradova LV, Perescis M, van Rijn CM, Sysoev IV. Revealing changes in directed interstructural couplingsat limbic seizures, induced by injection of cb1 receptor antagonist using nonlinear granger causality method. I.P. Pavlov Journal of Higher Nervous Activity. 2019;69(6):752–767 (in Russian). DOI: 10.1134/S0044467719060121.